

УДК 539.165

## STATUS OF $^{116}\text{Cd}$ DOUBLE $\beta$ DECAY STUDY WITH $^{116}\text{CdWO}_4$ SCINTILLATORS

*P. G. Bizzeti*<sup>b</sup>, *F. A. Danevich*<sup>a</sup>, *T. F. Fazzini*<sup>b</sup>, *A. Sh. Georgadze*<sup>a</sup>,  
*V. V. Kobychiev*<sup>a</sup>, *B. N. Kropivnyansky*<sup>a</sup>, *P. R. Maurenzig*<sup>b</sup>, *A. S. Nikolaiko*<sup>a</sup>,  
*O. A. Ponkratenko*<sup>a</sup>, *V. I. Tretyak*<sup>a</sup>, *S. Yu. Zdesenko*<sup>a</sup>, *Yu. G. Zdesenko*<sup>a</sup>

<sup>a</sup> Institute for Nuclear Research, MSP 03680 Kiev, Ukraine

<sup>b</sup> Dip. di Fisica, Università di Firenze and INFN, 50125 Firenze, Italy

A new set-up with four enriched  $^{116}\text{CdWO}_4$  scintillators with the mass of 0.34 kg is presented. The measured half-life for  $2\nu 2\beta$  decay as well as the  $T_{1/2}$  limits for different modes of neutrinoless  $2\beta$  decay of  $^{116}\text{Cd}$  are reported.

Представлена новая экспериментальная установка, состоящая из четырех сцинтилляторов  $^{116}\text{CdWO}_4$  с массой 0,34 кг. Приведены экспериментальные пределы для  $2\nu 2\beta$ - и безнейтринной мод распада  $^{116}\text{Cd}$ .

### INTRODUCTION

Neutrinoless ( $0\nu$ ) double  $\beta$  decay is forbidden in the Standard Model (SM) since it violates lepton number ( $L$ ) conservation. However many extensions of the SM incorporate  $L$  violating interactions and thus could lead to the  $0\nu 2\beta$  decay [1, 2]. Currently, besides conventional neutrino ( $\nu$ ) exchange mechanism, there are many other possibilities to trigger this process [2]. Therefore, at present  $0\nu 2\beta$  decay is considered as a powerful test of new physical effects beyond the SM, and even the absence of this process would help to restrict or narrow this wide choice of theoretical models.

With the aim to enlarge the number of  $2\beta$  decay candidate nuclides studied at a sensitivity comparable with that for  $^{76}\text{Ge}$  [3, 4] and  $^{136}\text{Xe}$  [5] (neutrino mass limit of 0.5–2 eV), cadmium tungstate crystal scintillators, enriched in  $^{116}\text{Cd}$  to 83%, were developed and exploited in  $^{116}\text{Cd}$  research [6, 7]. The measurements were carried out in the Solotvina Underground Laboratory in a salt mine 430 m underground ( $\simeq 1000$  m w.e.) [8]. In the first phase of the experiment only one  $^{116}\text{CdWO}_4$  crystal (121 g) was used. The background rate in the energy range 2.7–2.9 MeV ( $Q_{2\beta} = 2805$  keV [9]) was equal to  $\approx 0.6$  counts/y · kg · keV. With 19175 h statistics the half-life limit for  $0\nu 2\beta$  decay of  $^{116}\text{Cd}$  was set as  $T_{1/2}(0\nu) \geq 3.2 \cdot 10^{22}$  y (90% C.L.), which corresponds to the restriction on the neutrino mass  $m_\nu \leq 3.9$  eV [7]. Limits on  $0\nu 2\beta$  decay with emission of one (M1) or two (M2) Majorons were obtained, too:  $T_{1/2}(0\nu\text{M1}) \geq 1.2 \cdot 10^{21}$  y and  $T_{1/2}(0\nu\text{M2}) \geq 2.6 \cdot 10^{20}$  y (90% C.L.) [10].

In the present paper new and advanced results of  $^{116}\text{Cd}$  research obtained with the help of an upgraded apparatus are described.

## 1. NEW SET-UP WITH FOUR $^{116}\text{CdWO}_4$ DETECTORS

**1.1. Set-up and Measurements.** In the new apparatus four enriched  $^{116}\text{CdWO}_4$  crystals (total mass 339 g) are viewed by the PMT (EMI9390) through one light-guide 10 cm in diameter and 55 cm long, which is glued of two parts: quartz 25 cm long and plastic scintillator 30 cm long. The  $^{116}\text{CdWO}_4$  crystals are surrounded by an active shield made of 15 natural  $\text{CdWO}_4$  scintillators with total mass of 20.6 kg. The veto crystals are viewed — by a low background PMT ( $\varnothing 17$  cm) — through an active plastic light-guide ( $\varnothing 17 \times 49$  cm). In turn the whole array of  $\text{CdWO}_4$  counters is placed inside an additional active shield made of polystyrene-based plastic scintillator with dimensions  $40 \times 40 \times 95$  cm. Together with both active light-guides a complete  $4\pi$  active shield of the main  $^{116}\text{CdWO}_4$  detectors is provided.

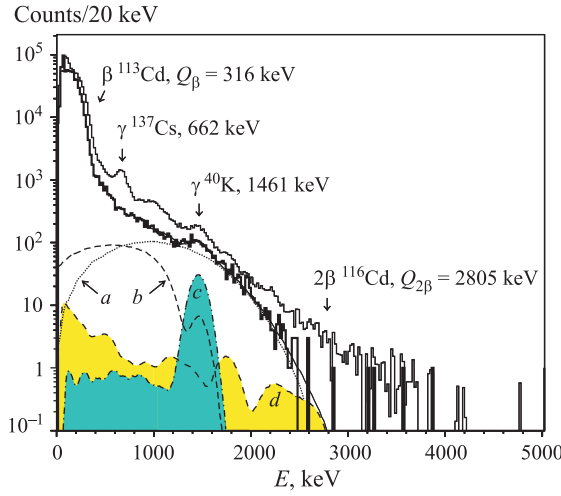


Fig. 1. Background spectrum of  $^{116}\text{CdWO}_4$  detectors (339 g) measured in the set-up with four enriched crystals during 4629 h (solid histogram). The old data obtained with one  $^{116}\text{CdWO}_4$  crystal (121 g; 19986 h) is shown for comparison (thin histogram; the data are normalized to 4629 h and mass of the new detector). The background components used for fit in the energy region 900–2900 keV: *a*)  $2\nu 2\beta$  decay of  $^{116}\text{Cd}$  (fit value is  $T_{1/2}(2\nu) = 2.6(1) \cdot 10^{19}$  y); *b*)  $^{40}\text{K}$  inside the  $^{116}\text{CdWO}_4$  detector (activity value from the fit is  $0.8(2)$  mBq  $\cdot$  kg $^{-1}$ ); *c*)  $^{40}\text{K}$  in the shielding  $\text{CdWO}_4$  crystals (fit value is  $2.1(3)$  mBq  $\cdot$  kg $^{-1}$ ); *d*)  $^{226}\text{Ra}$  and  $^{232}\text{Th}$  contamination of PMTs

The energy dependence of the resolution can be expressed as  $\text{FWHM}(\text{keV}) = \sqrt{-226 + 16.6E + 6.42 \cdot 10^{-3}E^2}$ , where energy  $E$  is in keV. Also, the relative light yield for  $\alpha$  particles as compared with that for electrons ( $\alpha/\beta$  ratio) and energy resolution were

The outer passive shield consists of HP copper (thickness 3–6 cm), lead (22.5–30 cm) and polyethylene (16 cm). Two plastic scintillators ( $120 \times 130 \times 3$  cm) are installed above the passive shield to provide a cosmic muons veto. The set-up is isolated carefully against air penetration. All materials used in the installation were previously tested and selected for low radioactive impurities in order to reduce their contributions to background.

The data acquisition system is based on two IBM personal computers (PC) and a CAMAC crate with electronic units. For each event the amplitude of a signal, its arrival time and the additional tags (the coincidence between different detectors; the signal of radio-noise detection system; triggers for light emitting diode (LED) and pulse shape digitizer) are stored on the hard disc of the first computer. The second computer records the pulse shape (in 2048 channels with a 50 ns channel's width) of the  $^{116}\text{CdWO}_4$  scintillators in the energy range 0.25–5 MeV.

The energy scale and resolution of the main detector were determined in the measurements with different  $\gamma$  sources ( $^{22}\text{Na}$ ,  $^{40}\text{K}$ ,  $^{60}\text{Co}$ ,  $^{137}\text{Cs}$ ,  $^{207}\text{Bi}$ ,  $^{226}\text{Ra}$ ,  $^{232}\text{Th}$ , and  $^{241}\text{Am}$ ).

measured with  $\alpha$  source ( $^{241}\text{Am}$ ) and corrected by using the time-amplitude analysis (see below) as following:  $\alpha/\beta = 0.15(1) + 7 \cdot 10^{-6} E_\alpha$  and  $\text{FWHM}_\alpha(\text{keV}) = 0.053 E_\alpha$  ( $E_\alpha$  is in keV). The routine calibration is carried out with a  $^{207}\text{Bi}$  and  $^{232}\text{Th}$   $\gamma$  sources. The dead time of the spectrometer and data acquisition is monitored permanently with the help of an LED optically connected to the main PMT. The actual dead time value is  $\approx 4.2\%$ .

The background spectrum measured during 4629 h with four  $^{116}\text{CdWO}_4$  crystals is given in Fig. 1, where the old data obtained with one  $^{116}\text{CdWO}_4$  crystal of 121 g are also shown for comparison. In the energy region 2.5–3.2 MeV the background rate is reduced to a value of 0.03 counts/y · kg · keV.

**1.2. Time-Amplitude Analysis of the Data.** The energy and arrival time of each event can be used for the analysis and selection of some decay chains in  $^{232}\text{Th}$ ,  $^{235}\text{U}$  and  $^{238}\text{U}$  families. As an example we consider here in detail the time-amplitude analysis of the following sequence

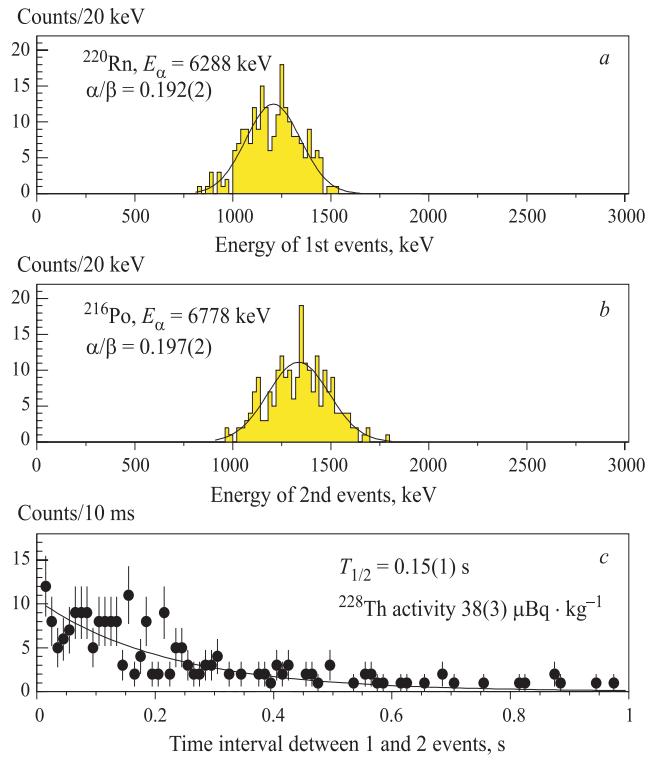


Fig. 2. The energy spectra of the first (a) and second (b)  $\alpha$  particles from the  $^{220}\text{Rn} \rightarrow ^{216}\text{Po} \rightarrow ^{212}\text{Pb}$  chain selected by time-amplitude analysis from  $^{116}\text{CdWO}_4$  data. Their equivalent energies in the  $\beta/\gamma$  energy scale are near 5 times smaller because the relative light yield for  $\alpha$  particles as compared with that for electrons ( $\alpha/\beta$  ratio) is  $\approx 0.2$ . c) Time distribution between the first and second events together with exponential fit ( $T_{1/2} = 0.15(1) \text{ s}$ , while the table value is  $T_{1/2} = 0.145(2) \text{ s}$  [16])

of  $\alpha$  decays from  $^{232}\text{Th}$  family:  $^{220}\text{Rn}$  ( $Q_\alpha = 6.40 \text{ MeV}$ ,  $T_{1/2} = 55.6 \text{ s}$ )  $\rightarrow$   $^{216}\text{Po}$  ( $Q_\alpha = 6.91 \text{ MeV}$ ,  $T_{1/2} = 0.145 \text{ s}$ )  $\rightarrow$   $^{212}\text{Pb}$ . The events in the energy region 0.7–1.8 MeV were used

as triggers. Then all events (within 0.9–1.9 MeV) following the triggers in the time interval 10–1000 ms were selected. The spectra of the  $^{220}\text{Rn}$  and  $^{216}\text{Po}$   $\alpha$  decays obtained in this way from data — as well as the distribution of the time intervals between the first and second events — are presented in Fig. 2. Using these results and taking into account the efficiency of the time-amplitude analysis and the number of accidental coincidences, the determined activity of  $^{228}\text{Th}$  ( $^{232}\text{Th}$  family) inside the  $^{116}\text{CdWO}_4$  crystals is as low as  $38(3) \mu\text{Bq} \cdot \text{kg}^{-1}$ .

The same technique was applied to the sequence of  $\alpha$  decays from the  $^{235}\text{U}$  family: ( $^{219}\text{Rn} \rightarrow ^{215}\text{Po}$  ( $T_{1/2} = 1.78 \text{ ms}$ )  $\rightarrow ^{211}\text{Pb}$ ) and sequence of  $\beta$  and  $\alpha$  decays from the  $^{238}\text{U}$  family:  $^{214}\text{Bi} \rightarrow ^{214}\text{Po}$  ( $T_{1/2} = 164.3 \mu\text{s}$ )  $\rightarrow ^{210}\text{Pb}$ . Activity of  $5.5(14) \mu\text{Bq} \cdot \text{kg}^{-1}$  for the  $^{227}\text{Ac}$  (the  $^{235}\text{U}$  family) and limit  $\leq 5 \mu\text{Bq} \cdot \text{kg}^{-1}$  for the  $^{226}\text{Ra}$  chain ( $^{238}\text{U}$  family) in the  $^{116}\text{CdWO}_4$  crystals were set. Finally, all couples of events found for  $^{232}\text{Th}$ ,  $^{235}\text{U}$  and  $^{238}\text{U}$  families were eliminated from the measured data.

**1.3. Pulse-Shape Discrimination.** Due to different shapes of scintillation signal for various kinds of sources ( $\alpha$  particles, protons,  $\gamma$  quanta and cosmic muons were investigated), the pulse-shape (PS) discrimination method based on the optimal digital filter [11] was developed and clear discrimination between  $\gamma$  rays (electrons) and  $\alpha$  particles was achieved [12].

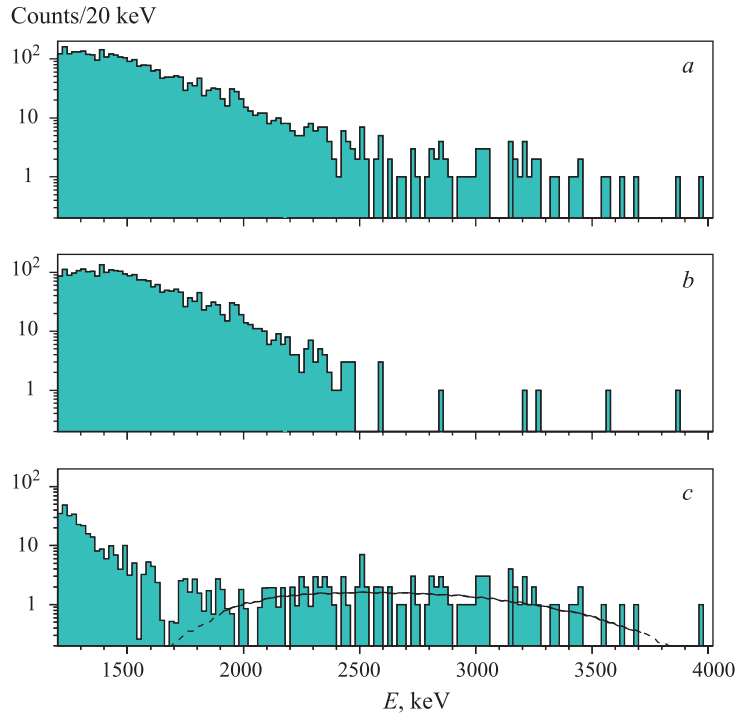


Fig. 3. *a*) Initial spectrum of  $^{116}\text{CdWO}_4$  crystals (339 g, 4629 h) in anticoincidence with shielding detectors without pulse-shape discrimination; *b*) PS selected  $\beta/\gamma$  events (see text); *c*) the difference between spectra in Figs. 3, *a* and 3, *b* together with the fit by the response function for  $^{212}\text{Bi} \rightarrow ^{212}\text{Po} \rightarrow ^{208}\text{Pb}$  decay chain. The fit value is  $37(4) \mu\text{Bq} \cdot \text{kg}^{-1}$  for  $^{228}\text{Th}$  activity inside  $^{116}\text{CdWO}_4$  crystals

The pulse shapes of enriched crystals were measured for  $\alpha$  particles with an  $^{241}\text{Am}$  source and for  $\gamma$  rays with  $^{60}\text{Co}$ ,  $^{137}\text{Cs}$ ,  $^{207}\text{Bi}$  and  $^{232}\text{Th}$  sources in the special calibration runs. The numerical characteristics of the pulse shape (shape indicator, SI, see for more details Ref. 12) are well described by a Gaussian functions, whose mean values and standard deviations  $\sigma_\alpha$  and  $\sigma_\gamma$  have a slight energy dependence<sup>1</sup>. It allows us to determine the efficiency of the PS event selection for the different chosen intervals of SI values. The PS selection technique ensures the very important possibility to discriminate «illegal» events: double pulses,  $\alpha$  events, etc., and thus to suppress background.

Since the shape indicator characterizes the full signal, it is also useful to examine the pulse front edge. For example, it was found that at least 99 % of «pure»  $\gamma$  events (measured with calibration  $^{232}\text{Th}$  source) satisfy the following restriction on pulse rise time:  $\Delta t(\mu\text{s}) \leq 1.24 - 0.5E_\gamma + 0.078E_\gamma^2$ , where  $E_\gamma$  is dimensionless variable expressed in MeV. Hence, this filter was applied to the background data, and all events, which do not pass the test, were excluded from the residual  $\beta/\gamma$  spectrum.

The results of PS analysis of the data are presented in Fig. 3. The initial (without PS selection) spectrum of the  $^{116}\text{CdWO}_4$  scintillators in the energy region 1.2–4 MeV — collected in anticoincidence with active shield — is depicted in Fig. 3, *a*, while the spectrum after PS selection of the  $\beta/\gamma$  events, whose SI lies in the interval  $\text{SI}_\gamma - 3.0\sigma_\gamma \leq \text{SI} \leq \text{SI}_\gamma + 2.4\sigma_\gamma$  and  $\Delta t(\mu\text{s}) \leq 1.24 - 0.5E_\gamma + 0.078E_\gamma^2$  (98 % of  $\beta/\gamma$  events), is shown in Fig. 3, *b*.

Further, Fig. 3, *c* represents the difference between spectra in Figs. 3, *a* and 3, *b*. These events, at least for the energy above 2 MeV, can be produced by  $^{228}\text{Th}$  activity from the intrinsic contamination of the  $^{116}\text{CdWO}_4$  crystals. Indeed, two decays in the fast chain  $^{212}\text{Bi}$  ( $Q_\beta = 2.25$  MeV)  $\rightarrow$   $^{212}\text{Po}$  ( $Q_\alpha = 8.95$  MeV,  $T_{1/2} = 0.3$   $\mu\text{s}$ )  $\rightarrow$   $^{208}\text{Pb}$  cannot be time resolved in the  $\text{CdWO}_4$  scintillator and will result in one event. To determine the residual activity of  $^{228}\text{Th}$  in the crystals, the response function of  $^{116}\text{CdWO}_4$  detectors for the  $^{212}\text{Bi} \rightarrow ^{212}\text{Po} \rightarrow ^{208}\text{Pb}$  chain was simulated with the help of

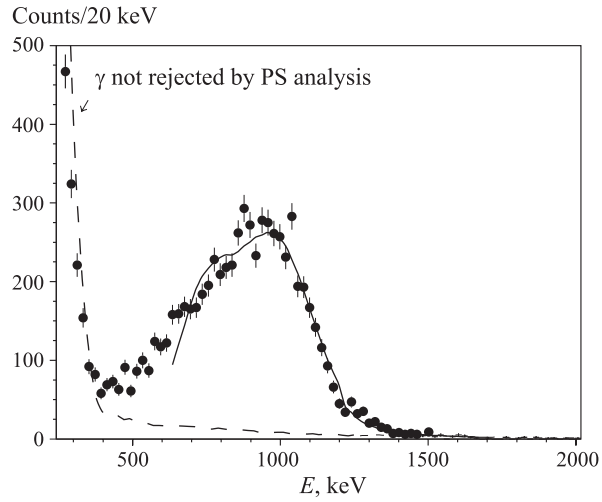


Fig. 4. Spectrum after PS selection of the background events, whose SI lies in the interval  $\text{SI}_\gamma + 2.4\sigma_\gamma < \text{SI} < \text{SI}_\alpha + 2.4\sigma_\alpha$  (it contains  $\approx 90\%$  of all  $\alpha$  events). The model distribution (smooth line) includes all  $\alpha$ -particles from chains in  $^{232}\text{Th}$  and  $^{238}\text{U}$  families. The total  $\alpha$  activity of the  $^{116}\text{CdWO}_4$  crystals is derived as  $1.4(3)$   $\text{mBq} \cdot \text{kg}^{-1}$

<sup>1</sup>For the  $\gamma$ -s (300–3200 keV)  $\text{SI}_\gamma = 18.09 - (4.5 \cdot 10^{-5} E_\gamma)$ ,  $\sigma_\gamma = 2.61 - (4.7 \cdot 10^{-4} E_\gamma) + 707/E_\gamma$ , while for the  $\alpha$  particles (4000–6000 keV)  $\text{SI}_\alpha = 29.0$ ;  $\sigma_\alpha = 5.11 - (5.52 \cdot 10^{-4} E_\alpha) + 5520/E_\alpha$ . Here all variables are dimensionless ( $E_\gamma$  and  $E_\alpha$  are expressed in keV).

GEANT3.21 code [13] and event generator DECAY4 [14]. The simulated function is shown in Fig. 3, *c*. The high energy part of the experimental spectrum is well reproduced ( $\chi^2 = 1.3$ ) by the expected response for  $^{212}\text{Bi} \rightarrow ^{212}\text{Po} \rightarrow ^{208}\text{Pb}$  decays<sup>1</sup>. Corresponding activity of  $^{228}\text{Th}$  inside the  $^{116}\text{CdWO}_4$  crystals, deduced from the fit in the 1.9–3.7 MeV energy region, is  $37(4) \mu\text{Bq} \cdot \text{kg}^{-1}$ , that is in good agreement with the value determined by the time-amplitude analysis of the chain  $^{220}\text{Rn} \rightarrow ^{216}\text{Po} \rightarrow ^{212}\text{Pb}$ . Besides, the front edge analysis of 80 events with the energy  $2.0\text{--}4.2$  MeV ( $\text{SI} \geq \text{SI}_\gamma + 2.54\sigma_\gamma$ ;  $\Delta t \geq 0.2 \mu\text{s}$ ) was fulfilled and the half-life derived from the average time delay between the first and second part of the signal is  $T_{1/2} = 0.31(6) \mu\text{s}$ , in agreement with the  $^{212}\text{Po}$  table value  $T_{1/2} = 0.299(2) \mu\text{s}$  [15].

Figure 4 represents the spectrum after PS selection of the background events, whose SI lies in the interval  $\text{SI}_\gamma + 2.4\sigma_\gamma < \text{SI} < \text{SI}_\alpha + 2.4\sigma_\alpha$  ( $\approx 90\%$  of  $\alpha$  events). The obtained distribution with maximum at 0.95 MeV is well reproduced by the model, which includes  $\alpha$  particles from chains in  $^{232}\text{Th}$  and  $^{238}\text{U}$  families (under assumption that secular radioactive equilibriums are broken). The total  $\alpha$  activity of the  $^{116}\text{CdWO}_4$  crystals deduced from Fig. 4 is  $1.4(3) \text{mBq} \cdot \text{kg}^{-1}$ .

## 2. RESULTS AND DISCUSSION

**2.1. Two-Neutrino Double Beta Decay of  $^{116}\text{Cd}$ .** To determine the half-life of two-neutrino  $2\beta$  decay of  $^{116}\text{Cd}$ , the background was simulated by the Monte Carlo method.

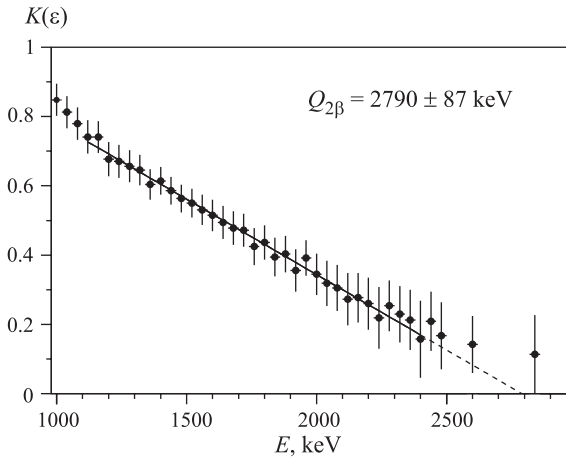


Fig. 5. The  $2\nu 2\beta$  decay Kurie plot and its fit by the straight line in 1100–2400 keV region

In addition to  $^{116}\text{Cd}$   $2\nu 2\beta$  decay distribution, only three components shown in Fig. 1 were used to build up the background model:  $^{40}\text{K}$  contamination of the enriched and natural  $\text{CdWO}_4$  scintillators and external  $\gamma$  background caused by  $^{232}\text{Th}$  and  $^{238}\text{U}$  contamination of the PMTs<sup>2</sup>. This simple background model describes experimental data in the energy interval 900–2900 keV reasonably well ( $\chi^2 = 1.3$ ) and gives the following results: the activities of  $^{40}\text{K}$  inside the enriched and natural  $\text{CdWO}_4$  crystals are equal to  $0.8(2)$  and  $2.1(3) \text{mBq} \cdot \text{kg}^{-1}$ , respectively; the half-life of two-neutrino  $2\beta$  decay of  $^{116}\text{Cd}$  is  $T_{1/2}(2\nu) = 2.6(1) \cdot 10^{19} \text{y}$ .

Taking advantage of the high statistics in our experiment (approximately 3600 events of  $^{116}\text{Cd}$  two-neutrino  $2\beta$  decay are

<sup>1</sup>The rest of spectrum below 1.9 MeV (Fig. 3, *c*) can be explained as high energy tail of the PS selected  $\alpha$  particles (see Fig. 4).

<sup>2</sup>The radioactive impurities of all PMTs used in the installation were previously measured by R&D low background set-up as (0.4–2.2) Bq/PMT and (0.1–0.2) Bq/PMT for  $^{226}\text{Ra}$  and  $^{228}\text{Th}$  activity, respectively [10].

contained within the interval 900–2900 keV), we can prove our model with the help of experimental  $2\nu2\beta$  decay Kurie plot:  $K(\varepsilon) = [S(\varepsilon) / \{(\varepsilon^4 + 10\varepsilon^3 + 40\varepsilon^2 + 60\varepsilon + 30)\varepsilon\}]^{1/5}$ , where  $S$  is the number of events with the energy  $\varepsilon$  (in electron mass units) in the experimental spectrum after background subtraction. For the real  $2\nu2\beta$  decay events such a Kurie plot should be the straight line  $K(\varepsilon) \sim (Q_{2\beta} - \varepsilon)$ , where  $Q_{2\beta}$  is the  $2\beta$  energy release. The experimental Kurie plot (Fig. 5) is well fitted in the region 1.1–2.4 MeV by the straight line with  $Q_{2\beta} = 2790(87)$  keV (table value is  $Q_{2\beta} = 2805(4)$  keV). Taking into account the energy resolution of the detector, fit in the energy region 1.2–2.8 MeV yields a very similar value  $Q_{2\beta} = 2779(52)$  keV and half-life corresponding to  $T_{1/2}(2\nu) = 2.5(3) \cdot 10^{19}$  y, thus justifying our assumption that experimental data in the region above 1.2 MeV are related mainly with  $^{116}\text{Cd}$  two-neutrino  $2\beta$  decay.

**Table 1. Different origins of the systematical uncertainties and their contributions to the half-life value of  $^{116}\text{Cd}$  two-neutrino  $2\beta$  decay**

Origin of the systematical error	Value range	Contribution to $T_{1/2}(2\nu)$ value, $10^{19}$ y
Life measuring time	$96_{-8}^{+2}$ %	+ 0.05, –0.2
Efficiency of PS analysis	$98_{-8}^{+1}$ %	+ 0.05, –0.3
Detection efficiency of $2\nu2\beta$ decay (GEANT model uncertainty)	$96 \pm 4$ %	$\pm 0.1$
$^{90}\text{Sr}$ – $^{90}\text{Y}$ impurity in $^{116}\text{CdWO}_4$	$\leq 0.17$ mBq $\cdot$ kg $^{-1}$	+ 0.5
$^{234m}\text{Pa}$ impurity in $^{116}\text{CdWO}_4$	$\leq 0.19$ mBq $\cdot$ kg $^{-1}$	+ 0.3

To estimate systematical uncertainties of the measured half-life, different origins of errors were taken into account, whose contributions are listed in the Table. The final value is equal to:

$$T_{1/2}(2\nu) = 2.6 \pm 0.1(\text{stat.})_{-0.4}^{+0.7}(\text{syst.}) \cdot 10^{19} \text{ y.}$$

Our result is in agreement with those measured earlier ( $T_{1/2}(2\nu) = 2.6_{-0.5}^{+0.9} \cdot 10^{19}$  y [16] and  $T_{1/2}(2\nu) = 2.7_{-0.4}^{+0.5}(\text{stat.})_{-0.6}^{+0.9}(\text{syst.}) \cdot 10^{19}$  y [6]) and disagrees to some extent with the value  $T_{1/2}(2\nu) = 3.75 \pm 0.35(\text{stat.}) \pm 0.21(\text{syst.}) \cdot 10^{19}$  y from Ref. 17<sup>1</sup>.

**2.2. New Limits for  $0\nu2\beta$  Decay of  $^{116}\text{Cd}$ .** The high energy part of the experimental spectrum of the  $^{116}\text{CdWO}_4$  crystals measured in anticoincidence with the shielding detectors and after the time-amplitude and pulse-shape selection is shown in Fig. 6.

The peak of  $0\nu2\beta$  decay is absent, thus from the data we obtain a lower limit of the half-life:  $\lim T_{1/2} = \ln 2N\eta t / \lim S$ , where  $N = 4.66 \cdot 10^{23}$  is the number of  $^{116}\text{Cd}$  nuclei;  $t$  is the measuring time ( $t = 4629$  h);  $\eta$  is the total detection efficiency for  $0\nu2\beta$  decay, and  $\lim S$

<sup>1</sup>Note, that in [17] the quite small detection efficiency (1.73 %) was calculated by the Monte Carlo method without experimental test, thus perhaps systematical error could be higher than the quoted value.

is the number of events in the peak which can be excluded with a given confidence level. The value of the detection efficiency  $\eta_{MC} = 0.83$  was calculated by the DECA4 and GEANT3.21 codes, while the efficiency of the PS analysis  $\eta_{PS} = 0.98$  was determined as described above, thus the total efficiency  $\eta = \eta_{MC} \cdot \eta_{PS} = 0.81$ . To estimate  $\lim S$  energy interval 2.6–3.1 MeV (containing 91 % of  $0\nu 2\beta$  peak, where there is only one measured event) was considered. The expected background in the same energy region is  $3.2^{+2.1}_{-1.1}$  counts ( $1.9 \pm 0.7$  events from PMT contamination;  $0.4 \pm 0.1$  events from  $2\nu 2\beta$  distribution;  $0.9^{+2}_{-0.9}$  counts from mentioned  $^{212}\text{Bi} \rightarrow ^{212}\text{Po} \rightarrow ^{208}\text{Pb}$  chain). Following the PDG recommendation [18, 19] we can derive from these numbers the excluded limit as  $\lim S = 1.8(0.5)$  with 90 % (68 %) C.L., which leads to half-life limits for neutrinoless  $2\beta$  decay of  $^{116}\text{Cd}$ :

$$T_{1/2}(0\nu 2\beta) \geq 0.7(2.5) \cdot 10^{23} \text{ y}, \quad 90 \% (68 \%) \text{ C.L.}$$

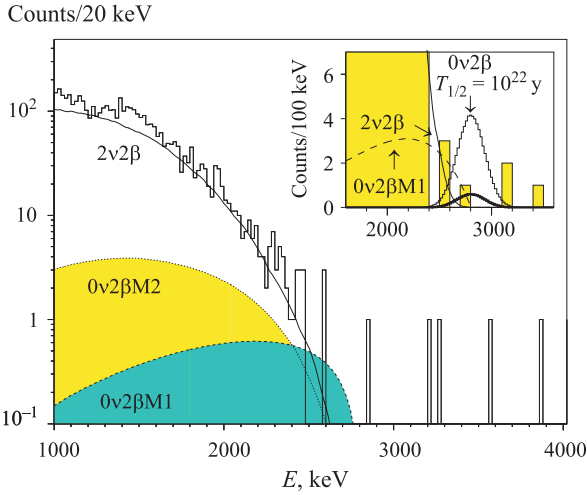


Fig. 6. Part of experimental spectrum of the  $^{116}\text{CdWO}_4$  detectors measured during 4629 h (histogram) together with the fit from  $2\nu 2\beta$  contribution ( $T_{1/2} = 2.6 \cdot 10^{19}$  y). The smooth curves  $0\nu 2\beta\text{M1}$  and  $0\nu 2\beta\text{M2}$  are excluded with 90 % C.L. distributions of  $0\nu\text{M1}$  and  $0\nu\text{M2}$  decay of  $^{116}\text{Cd}$  with  $T_{1/2} = 3.7 \cdot 10^{21}$  y and  $T_{1/2} = 5.9 \cdot 10^{20}$  y, respectively. In the insert the expected peak from  $0\nu 2\beta$  decay with  $T_{1/2}(0\nu) = 1.0 \cdot 10^{22}$  y is shown together with the excluded (90 % C.L.) distribution (solid histogram) with  $T_{1/2}(0\nu) = 7.0 \cdot 10^{22}$  y

the help of GEANT3.21 and DECA4 codes full peak efficiencies for  $0\nu 2\beta$  decay to the first and second excited levels of  $^{116}\text{Sn}$  ( $2_1^+$  with  $E_{\text{lev}} = 1294$  keV and  $0_1^+$  with  $E_{\text{lev}} = 1757$  keV) are:  $\eta(2_1^+) = 0.14$  and  $\eta(0_1^+) = 0.07$ . These numbers and the value of  $\lim S = 1.8(0.5)$  with 90 % (68 %) C.L. (determined for the g.s.  $\rightarrow$  g.s. transition) give the following restrictions on half-lives of  $^{116}\text{Cd}$  neutrinoless  $2\beta$  decay to excited levels of  $^{116}\text{Sn}$ :

Using calculations [20], one can obtain restrictions on the neutrino mass and right-handed admixtures in the weak interaction:  $m_\nu \leq 3.0$  eV,  $\eta \leq 3.9 \cdot 10^{-8}$ ,  $\lambda \leq 3.4 \cdot 10^{-6}$  at 90 % C.L., and neglecting right-handed contribution  $m_\nu \leq 2.6(1.4)$  eV at 90 % (68 %) C.L. On the basis of calculations [17] we get a similar result:  $m_\nu \leq 2.4(1.3)$  eV at 90 % (68 %) C.L. In accordance with Ref. 21 the value of the  $R$ -parity violating parameter of minimal SUSY standard model is restricted by our  $T_{1/2}$  limit to  $\varepsilon \leq 8.8(6.4) \cdot 10^{-4}$  at 90 % (68 %) C.L. (calculations [22] give more stringent restrictions:  $\varepsilon \leq 3.4(2.4) \cdot 10^{-4}$ ).

Excited levels of  $^{116}\text{Sn}$  with  $E_{\text{lev}} \leq Q_{2\beta}$  can be also populated in  $0\nu 2\beta$  decay of  $^{116}\text{Cd}$ . In this case one or several  $\gamma$  quanta, conversion electrons and/or  $e^+e^-$  pairs will be emitted in a deexcitation process, in addition to two electrons emitted in  $2\beta$  decay. The full absorption of all emitted particles should result in the peak with  $E = Q_{2\beta}$ . Calculated with

$$\begin{aligned} T_{1/2}(\text{g.s.} \rightarrow 2_1^+) &\geq 1.3(4.8) \cdot 10^{22} \text{ y}, & 90\% (68\%) \text{ C.L.}, \\ T_{1/2}(\text{g.s.} \rightarrow 0_1^+) &\geq 0.7(2.4) \cdot 10^{22} \text{ y}, & 90\% (68\%) \text{ C.L.} \end{aligned}$$

To obtain half-life limits for  $0\nu 2\beta$  decay with one (two) Majoron(s) emission the measured spectrum was fitted in the energy region 1.6–2.8 MeV for  $0\nu\text{M1}$  mode (1.6–2.6 MeV for  $0\nu\text{M2}$ ) by using only three theoretical distributions:  $\gamma$  background from measured PMT-s contamination ( $^{226}\text{Ra}$  and  $^{232}\text{Th}$  chains) and two-neutrino  $2\beta$  decay of  $^{116}\text{Cd}$ , as background, and  $0\nu 2\beta$  decay with one (two) Majoron(s) emission, as effect. With this simple model the  $\chi^2$  value was equal to 1.1 both for  $0\nu\text{M1}$  and  $0\nu\text{M2}$  fits. As a result, the number of events under a theoretical  $0\nu\text{M1}$  curve was determined as  $9 \pm 21$ , giving no statistical evidence for the effect. It leads to an upper limit of 41(26) events at 90% (68%) C.L., that together with an efficiency value  $\eta = 0.905$  corresponds to the half-life limit:

$$T_{1/2}(0\nu\text{M1}) \geq 3.7(5.9) \cdot 10^{21} \text{ y}, \quad 90\% (68\%) \text{ C.L.}$$

A similar procedure for  $0\nu 2\beta$  decay with two Majorons emission gives:

$$T_{1/2}(0\nu\text{M2}) \geq 5.9(9.4) \cdot 10^{20} \text{ y}, \quad 90\% (68\%) \text{ C.L.}$$

Both the present half-life limits are more stringent than those established in our previous measurement during 19986 h [10] and in the NEMO experiment [17].

The probability of neutrinoless  $2\beta$  decay with Majoron emission can be expressed as:  $\{T_{1/2}(0\nu\text{M1})\}^{-1} = \langle g_M \rangle^2 |\text{NME}|^2 G$ , where  $\langle g_M \rangle$  is the effective Majoron-neutrino coupling constant, NME is the nuclear matrix element and  $G$  is the kinematical factor. Using our result  $T_{1/2}(0\nu\text{M1}) \geq 3.7(5.9) \cdot 10^{21}$  y and values of  $G$  and NME calculated in the QRPA model with proton-neutron pairing [23] we obtain  $g_M \leq 12(9.5) \cdot 10^{-5}$  ( $g_M \leq 6.5(5.4) \cdot 10^{-5}$  on the basis of calculation [17]) with 90% (68%) C.L., which is one of the best restriction up-to-date obtained in the direct  $2\beta$  decay experiments [1].

## CONCLUSION

The new set-up with four  $^{116}\text{CdWO}_4$  crystals (339 g) is running since October 1998 in the Solotvina Underground Laboratory. Improved passive shield, new active shield made of fifteen  $\text{CdWO}_4$  crystals (total mass 20.6 kg), as well as time-amplitude and pulse-shape analysis of the data result in the reduction of the background rate in the 2.5–3.2 MeV region to 0.03 counts/y · kg · keV. For 4629 h of the exposition the half-life for  $2\nu 2\beta$  decay of  $^{116}\text{Cd}$  is measured as  $T_{1/2}(2\nu) = 2.6 \pm 0.1(\text{stat.})_{-0.4}^{+0.7}(\text{syst.}) \cdot 10^{19}$  y. The  $T_{1/2}$  limits for neutrinoless  $2\beta$  decay of  $^{116}\text{Cd}$  are set at  $T_{1/2} \geq 0.7(2.5) \cdot 10^{23}$  y at 90% (68%) C.L. for transition to ground state of  $^{116}\text{Sn}$ , while for decays to the first  $2_1^+$  and second  $0_1^+$  excited levels of  $^{116}\text{Sn}$  at  $T_{1/2} \geq 1.3(4.8) \cdot 10^{22}$  y and  $\geq 0.7(2.4) \cdot 10^{22}$  y with 90% (68%) C.L., respectively. For  $0\nu 2\beta$  decay with emission of one or two Majorons, the limits are  $T_{1/2}(0\nu\text{M1}) \geq 3.7(5.8) \cdot 10^{21}$  y and  $T_{1/2}(0\nu\text{M2}) \geq 5.9(9.4) \cdot 10^{20}$  y at 90% (68%) C.L. Restrictions on the value of the neutrino mass, right-handed admixtures in the weak interaction, and the neutrino-Majoron coupling constant are derived as:  $m_\nu \leq 2.6(1.4)$  eV,  $\eta \leq 3.9 \cdot 10^{-8}$ ,  $\lambda \leq 3.4 \cdot 10^{-6}$ , and  $g_M \leq 12(9.5) \cdot 10^{-5}$  at 90% (68%) C.L., respectively [24].

In August 1999 one of our  $^{116}\text{CdWO}_4$  crystals was annealed at high temperature, and its light output has increased by  $\approx 13\%$ . The PMT of the main  $^{116}\text{CdWO}_4$  detectors was changed by a special low background EMI tube with the RbCs photocathode, whose spectral response better fits the  $\text{CdWO}_4$  scintillation light. As a result, the spectrometric parameters of the detector were improved. In particular, the energy resolution of the main detector is now  $11.4\%$  at  $1064\text{ keV}$  and  $8.6\%$  at  $2615\text{ keV}$  (comparing with those before this upgrading:  $14.5\%$  and  $11\%$ ). Besides, the PS discrimination ability of the detector was improved, too. It is expected that after approximately 5 years of measurements the half-life limit  $T_{1/2}(0\nu 2\beta) \geq 4 \cdot 10^{23}\text{ y}$  will be reached which corresponds to  $m_\nu \leq 1.2\text{ eV}$ . The bounds on neutrinoless  $2\beta$  decay with Majorons emission and  $2\beta$  transitions to the excited levels of  $^{116}\text{Sn}$  would be improved, too.

The present research was supported in part by the Ukraine Fundamental Researches Foundation (Grant F5/1930-98).

## REFERENCES

1. *Moe M., Vogel P.* // *Ann. Rev. Nucl. Part. Sci.* 1994. V. 44. P. 247;  
*Tretyak V. I., Zdesenko Yu. G.* // *At. Data Nucl. Data Tables.* 1995. V. 61. P. 43.
2. *Klapdor-Kleingrothaus H. V.* // *Int. J. Mod. Phys. A.* 1998. V. 13. P. 3953;  
*Suhonen J., Civitarese O.* // *Phys. Rep.* 1998. V. 300. P. 123;  
*Faessler A., Simkovic F. J.* // *Phys. G: Nucl. Part. Phys.* 1998. V. 24. P. 2139.
3. *Baudis L. et al.* // *Phys. Rev. Lett.* 1999. V. 83. P. 41.
4. *Aalseth C. E. et al.* // *Phys. Rev. C.* 1999. V. 59. P. 2108.
5. *Luescher R. et al.* // *Phys. Lett. B.* 1998. V. 434. P. 407.
6. *Danevich F. A. et al.* // *Phys. Lett. B.* 1995. V. 344. P. 72;  
*Georgadze A. Sh. et al.* // *Phys. At. Nucl.* 1995. V. 58. P. 1093.
7. *Danevich F. A. et al.* // *Nucl. Phys. B. (Proc. Suppl.)*. 1999. V. 70. P. 246.
8. *Zdesenko Yu. G. et al.* // *Proc. of the 2 Intern. Symp. Underground Phys., Baksan Valley, 1987. M., 1988.* P. 291.
9. *Audi G., Wapstra A. H.* // *Nucl. Phys. A.* 1995. V. 595. P. 409.
10. *Danevich F. A. et al.* // *Nucl. Phys. A.* 1998. V. 643. P. 317.
11. *Gatti E., Martini F.* // *De Nuclear Electronics 2, IAEA. Vienna, 1962.* P. 265.
12. *Fazzini T. et al.* // *Nucl. Instr. Meth. A.* 1998. V. 410. P. 213.
13. GEANT. CERN Program Library Long Write-up W5013. CERN, 1994.
14. *Ponkratenko O. A. et al.* // *Proc. of the Intern. Conf. on Non-Accelerator New Physics NANP'99, Dubna, June 28–July 3, 1999.* To be published in «*Phys. At. Nucl.*».
15. *Firestone R. B.* *Table of Isotopes / Ed. by V. S. Shirley.* 8th ed. N.Y., 1996.
16. *Ejiri H. et al.* // *J. Phys. Soc. Japan.* 1995. V. 64. P. 339.
17. *Arnold R. et al.* // *Z. Phys. C.* 1996. V. 72. P. 239.
18. Particle Data Group. *Review of Particle Physics* // *Eur. Phys. J. C.* 1998. V. 3. P. 1.

19. Feldman G.J., Cousins R.D. // Phys. Rev. D. 1998. V.57. P.3873.
20. Staudt A. et al. // Europhys. Lett. 1990. V. 13. P. 31.
21. Hirsch M. et al. // Phys. Rev. D. 1996. V.53. P.1329.
22. Faessler A. et al. // Phys. Rev. D. 1998. V. 58. P. 115004.
23. Hirsch M. et al. // Phys. Lett. B. 1996. V.372. P. 8.
24. Danevich F.A. et al. // Phys. Rev. C. 2000. V. 62. P. 045501.